A Translocated Bacterial Protein Protects Vascular Endothelial Cells from Apoptosis

Michael C. Schmid[1], Florine Scheidegger[1], Michaela Dehio[1], Nadège Balmelle-Devaux[1], Ralf Schulein[1], Patrick Guye[1], Cuddapah S. Chennakesava[2], Barbara Biedermann[2], Christoph Dehio[1*]

1 Division of Molecular Microbiology, Biozentrum, University of Basel, Basel, Switzerland, 2 Department of Research, University Hospital, Basel, Switzerland

The modulation of host cell apoptosis by bacterial pathogens is of critical importance for the outcome of the infection process. The capacity of *Bartonella henselae* and *B. quintana* to cause vascular tumor formation in immunocompromised patients is linked to the inhibition of vascular endothelial cell (EC) apoptosis. Here, we show that translocation of BepA, a type IV secretion (T4S) substrate, is necessary and sufficient to inhibit EC apoptosis. Ectopic expression in ECs allowed mapping of the anti-apoptotic activity of BepA to the Bep intracellular delivery domain, which, as part of the signal for T4S, is conserved in other T4S substrates. The anti-apoptotic activity appeared to be limited to BepA orthologs of *B. henselae* and *B. quintana* and correlated with (i) protein localization to the host cell plasma membrane, (ii) elevated levels of intracellular cyclic adenosine monophosphate (cAMP), and (iii) increased expression of cAMP-responsive genes. The pharmacological elevation of cAMP levels protected ECs from apoptosis, indicating that BepA mediates anti-apoptosis by heightening cAMP levels by a plasma membrane–associated mechanism. Finally, we demonstrate that BepA mediates protection of ECs against apoptosis triggered by cytotoxic T lymphocytes, suggesting a physiological context in which the anti-apoptotic activity of BepA contributes to tumor formation in the chronically infected vascular endothelium.

Citation: Schmid MC, Scheidegger F, Dehio M, Balmelle-Devaux N, Schulein R, et al. (2006) A translocated bacterial protein protects vascular endothelial cells from apoptosis. PLoS Pathog 2(11): e115. doi:10.1371/journal.ppat.0020115

Introduction

Bacterial pathogens have developed various strategies to subvert host cell functions to their benefit. In particular, intracellular bacteria have adapted mechanisms to modulate the apoptotic pathway of their host cells [1]. The resulting induction or inhibition of apoptosis is often crucial for a successful infection of the host. Pathogen-induced apoptosis can serve to eliminate key immune cells or to evade other host defenses [1]. Several bacteria elicit an inflammatory process by inducing a specific form of apoptotic cell death, which at the place of infection leads to the disruption of tissue barriers and thus may secure efficient microbial spread in the host [2,3]. In contrast, inhibition of apoptosis may be essential for intracellular pathogens to establish chronic infection. Pathogen-triggered anti-apoptosis of infected host cells facilitates a slow microbial replication process and enables persistence in the infected host. For example, the obligate intracellular pathogen *Chlamydia pneumoniae* degrades—by an unknown effector mechanism—pro-apoptotic BH-3 host cell proteins [4]. *Rickettsia rickettsii* protects invaded host cells from apoptosis by activating a nuclear factor kappa B (NFκB)–dependent survival pathway [5]. For many human pathogens, the activation and inhibition of the apoptotic machinery of the infected host cell thus has a central role during the infection process [1].

The bacterial effectors known to modulate apoptosis are mostly pro-apoptotic. The only described anti-apoptotic effector is the outer membrane protein PorB of *Neisseria meningitidis* [6]. PorB has been shown to interact with mitochondria, where it is thought to block apoptosis by preventing mitochondrial depolarization and cytochrome C release. Interestingly, opposite effects were reported for the PorB ortholog of *N. gonorrhoea*, which provokes a pro-apoptotic effect upon interaction with mitochondria [7,8].

Bartonellae are facultative intracellular pathogens associated with the formation of vasoproliferative tumors in humans (e.g., bacillary angiomatosis, bacillary peliosis, and verruga peruana) [9]. These vascular lesions consist of an increased number of endothelial cells (ECs), which are colonized by extracellular and intracellular bacteria. Although at least nine *Bartonella* species are known to infect humans, vascular proliferation is mainly caused by the species *Bartonella henselae (Bh), B. quintana (Bq),* and *B. bacilliformis* [9]. Upon EC infection in vitro, *Bh* and *Bq* are able to stimulate proliferation and inhibition of apoptosis [9–11]. The anti-apoptotic activity of bartonellae is considered to contribute

Editor: Pascale Cossart, Institut Pasteur, France

Received January 17, 2006; **Accepted** September 19, 2006; **Published** November 24, 2006

Abbreviations: aa, amino acids; AC, adenylate cyclase; *Bh, Bartonella henselae;* BID, Bep intracellular delivery; *Bq, Bartonella quintana; Bt, Bartonella tribocorum;* Cya, calmodulin-dependent adenylate cyclase; cAMP, cyclic adenosine monophosphate; CFSE, carboxyfluorescein diacetate succinimidyl ester; CTL, cytotoxic T lymphocyte; CRAfT, Cre-recombinase assay for translocation; EC, endothelial cell; FIC, filamentation induced by cyclic adenosine monophosphate; GFP, green fluorescent protein; HUVEC, human umbilical vein endothelial cell; IBMX, 3-isobityl-1-methylxanthine; IL-8, interleukin 8; IPTG, isopropyl β-d-thiogalactosidase; MHC, major histocompatibility complex; MOI, multiplicity of infection; NFκB, nuclear factor kappa B; PI, propidium iodide; SD, standard deviation; T4S, type IV secretion; WGA, wheat germ agglutinin

* To whom correspondence should be addressed. E-mail: christoph.dehio@unibas.ch

Synopsis

The capacity of infected host cells to die by apoptosis (programmed cell death) is critical for controlling pathogen replication and survival. Bacterial pathogens have thus developed strategies to inhibit host cell apoptosis, allowing them to preserve their cellular habitat during chronic infection. For instance, the capacity of the facultative intracellular pathogen *Bartonella henselae* to trigger tumor formation as a consequence of chronic infection of the human vasculature is linked to the inhibition of endothelial cell apoptosis. This study describes the identification and functional characterization of the anti-apoptotic bacterial effector protein BepA of *B. henselae,* which is shown to be sufficient to inhibit endothelial cell apoptosis, i.e., as triggered by activated cytotoxic T lymphocytes. Upon translocation into endothelial cells via a bacterial type IV secretion system, BepA localizes to the plasma membrane, where it triggers the production of second messenger cyclic adenosine monophosphate in quantities effective for blocking apoptosis. Strikingly, the capacity of BepA to mediate membrane localization, cyclic adenosine monophosphate production, and the resulting inhibition of apoptosis is confined to a conserved domain that originally evolved in bacteria as a signal for type IV secretion. This study thus highlights the convergent evolution of an anti-apoptotic effector protein of purely bacterial origin.

synergistically to an unrelated mitogenic activity and results in the formation of vascular tumors [10,11].

In *Bh*, inhibition of apoptosis is dependent on a functional VirB/VirD4 system [12,13]. This type IV secretion (T4S) system is a major virulence determinant for *Bartonella*–EC interaction [12–14]. T4S systems are versatile transporters ancestrally related to bacterial conjugation machines. Different human pathogens have recruited such conjugation machineries to inject macromolecular effectors across the bacterial and host cell membranes directly into the host cell cytosol, where they alter various cellular processes [15]. *Bh* carries a pathogenicity island that encodes next to the *virB/virD4* locus seven putative T4S substrates, the *Bartonella*-translocated effector proteins *Bh* BepA–G [13]. Deletion of the pathogenicity island regions encoding *bepA–G* abolishes the anti-apoptotic activity and all other VirB/VirD4-dependent EC phenotypes [13]. However, the contribution of individual *Bh* Beps to anti-apoptosis and the other cellular phenotypes is unknown. All seven *Bh* Beps carry in their C-terminus at least one conserved region, called the Bep intracellular delivery (BID) domain [13]. The positively charged C-terminal tail sequence together with the proximal BID domain constitute a bipartite signal for T4S. Based on a Cre-recombinase assay for translocation (CRAfT), this T4S signal was shown to be functional for VirB/VirD4-dependent transfer of four different *Bh* Beps (*Bh* BepB, *Bh* BepC, *Bh* BepD, and *Bh* BepF) [13]. Evidence for translocation of *Bh* BepA, *Bh* BepE, and *Bh* BepG is still missing.

Bh BepA, *Bh* BepB, and *Bh* BepC are paralogous proteins. A *Bh* BepA ortholog is found in the animal pathogen *B. tribocorum (Bt)* [16]. Remarkably, all BepA homologs encode in their N-terminal part a conserved FIC (filamentation induced by cyclic adenosine monophosphate [cAMP]) domain, which was proposed to be involved in bacterial cell division [17], while the putative effector function within human cells is unknown.

In this paper, we identify BepA as anti-apoptotic effector of the vasoproliferative bartonellae *Bh* and *Bq*. We show that this effector is translocated by the VirB/VirD4 system into ECs. Further, we show that the anti-apoptotic activity is confined to the BID domain of *Bh* BepA, which also mediates localization to the EC plasma membrane. We demonstrate that *Bh* BepA provokes an elevation of intracellular cAMP and the upregulation of cAMP-responsive genes, suggesting that plasma membrane–associated *Bh* BepA triggers cAMP production and signaling, resulting in the abrogation of apoptotic processes. Accordingly, we were able to mimic the anti-apoptotic effect of BepA by artificially increasing the intracellular cAMP level in ECs. Finally, we demonstrate that BepA can inhibit cytotoxic T lymphocyte (CTL)–mediated apoptosis of ECs.

Results

Bh BepA Mediates Anti-Apoptosis in ECs

The anti-apoptotic activity of *Bh* on human umbilical vein endothelial cells (HUVECs) requires a functional VirB/VirD4 system and at least one of the putatively secreted effectors *Bh* BepA–G [12,13]. To identify the effector(s) required for inhibition of apoptosis, we expressed them individually in the substrate-free *bepA–G* mutant and assayed for anti-apoptotic activity. To this end, HUVECs were infected with the different *Bh* strains and apoptosis was induced by exposure to actinomycin D. Morphological examination (Figure 1A), measuring of caspase-3/-7 activity (Figure 1B), and flow cytometric analysis of Annexin V– and propidium iodide (PI)–stained cells (Figure 1C) were used to monitor apoptosis. Δ*bepA–G* did not display anti-apoptotic activity as reported previously [13]. Strikingly, the expression of *Bh* BepA (by plasmid p*Bh* BepA) restored the anti-apoptotic activity to wild-type level (Figure 1), whereas no other *Bh* Bep interfered with actinomycin D–triggered apoptosis (unpublished data). Consistently, strain Δ*bepA* carrying an in-frame deletion of *bepA* did not protect HUVECs from apoptosis, whereas complementation of this mutant with p*Bh* BepA restored the anti-apoptotic activity (Figure 1). To test for functionality of the VirB/VirD4 system in the Δ*bepA* mutant, we monitored the T4S-dependent process of invasome formation [12,18], and furthermore quantified the translocation efficiency of a reporter substrate (encoded by pRS51) using CRAfT [13]. Both assays confirmed that the VirB/VirD4 T4S system is functional in the Δ*bepA* strain (unpublished data).

Taken together, these results provide evidence that *Bh* requires the putative T4S substrate *Bh* BepA to protect HUVECs from apoptosis.

Bh BepA Is a VirB/VirD4 Substrate Translocated into ECs

CRAfT was used to demonstrate functionality of most of the C-terminal bipartite T4S signals of *Bh* Beps [13], while this assay was negative for the putative T4S substrate *Bh* BepA (unpublished data). Here, we adapted the calmodulin-dependent adenylate cyclase (Cya) reporter assay [19,20] as an alternative to test for translocation of *Bh* BepA into HUVECs. Translocation of a Cya reporter fusion is demonstrated by the increase in the intracellular cAMP level. An N-terminal FLAG-tag epitope was fused to Cya to determine the stability of fusion proteins by immunoblot analysis (Figure 2A and 2C). As positive control, the T4S signal of *Bh* BepD (*Bh* $BepD_{352–534}$) [13] was fused to the FLAG-Cya reporter

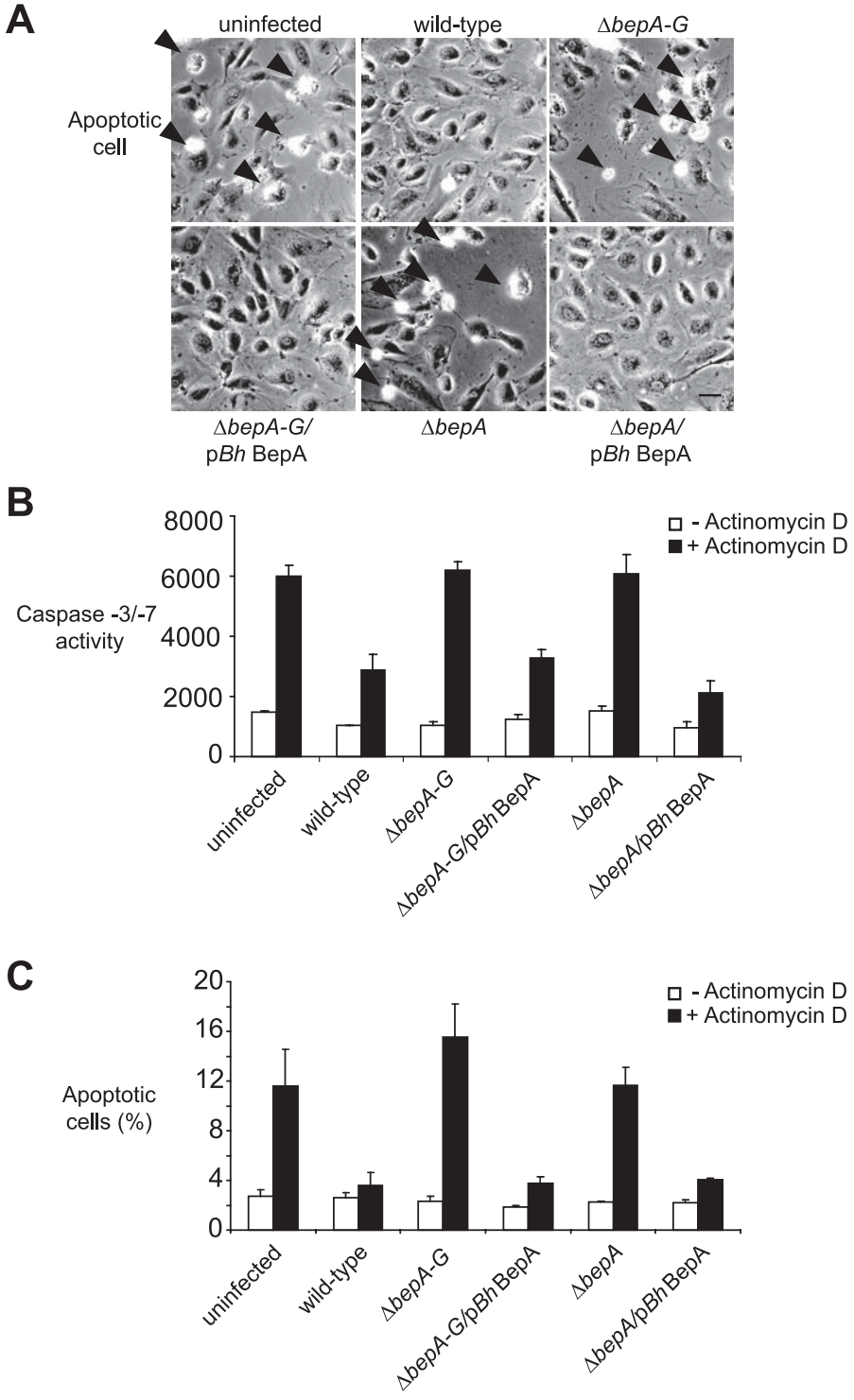

Figure 1. *Bh* BepA Meditates Inhibition of Apoptosis in ECs

(A and B) HUVECs were infected for 24 h with the indicated *Bh* strains (MOI = 300) or left uninfected for this period (control). If not indicated differently, apoptosis was then triggered by the addition of actinomycin D. Then, 12 h later, (A) morphological changes were visualized by recording phase contrast images (bar = 40 μm), and (B) caspase-3/-7 activities were determined with a specific fluorogenic peptide substrate. Arrowheads (A) indicate apoptotic cells displaying membrane blebbing.

(C) Twenty-four hours after induction of apoptosis, the loss of membrane asymmetry was quantified by flow cytometric analysis of AlexaFluor488 Annexin V– and PI-stained cells, allowing us to quantify the rate of apoptotic cells (Annexin V–positive and PI-negative). Mean and standard deviation (SD) are shown for one representative out of three independent replica experiments. All strains were tested a minimum of three times in triplicate samples.

doi:10.1371/journal.ppat.0020115.g001

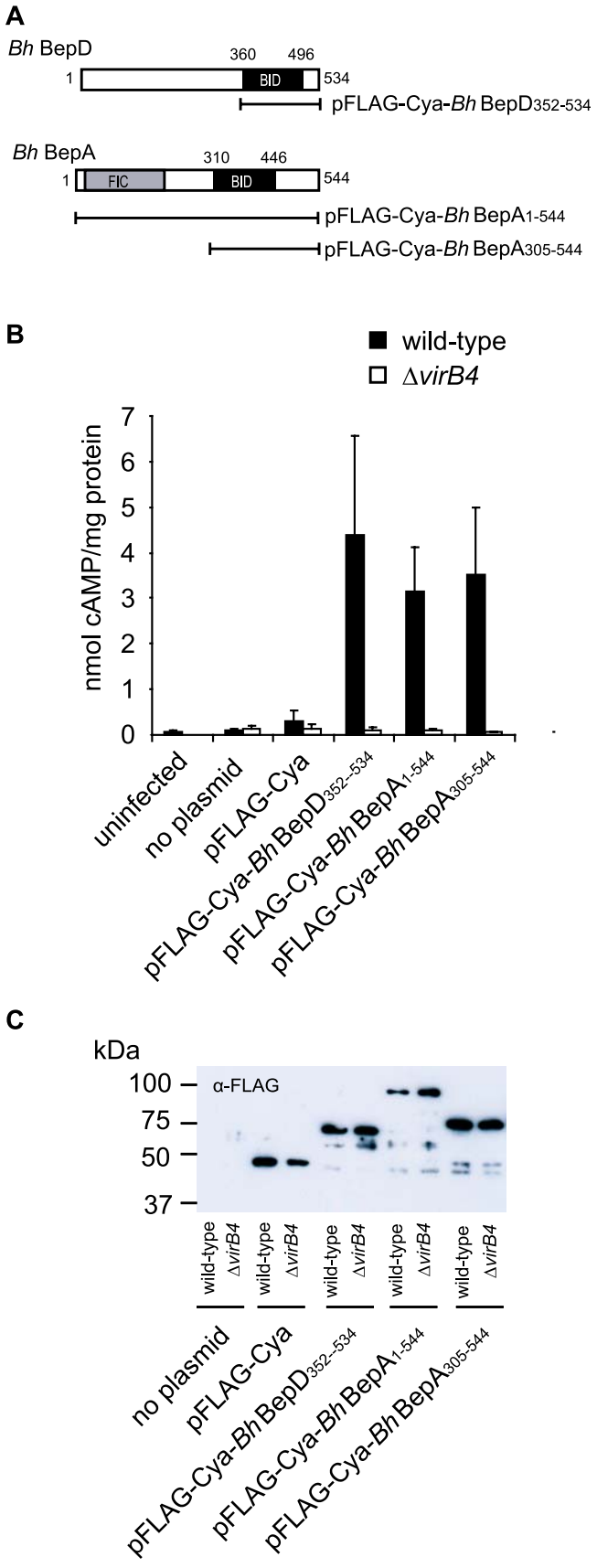

Figure 2. *Bh* BepA Is a Genuine VirB/VirD4 T4S Substrate That Is Translocated into ECs

(A) The bars indicate the parts of *Bh* BepA or *Bh* BepD that were fused to Cya. These reporter fusions were used to monitor translocation via the VirB/VirD4 system. All constructs contain an N-terminal FLAG epitope for immunological detection of the encoded fusion protein.

(B) Quantification of the amount of intracellular cAMP in HUVECs infected for 20 h with the indicated bacterial strains (MOI = 300). Isogenic strains with a functional (wild-type) or non-functional (Δ*virB4*) VirB/VirD4 T4S system were used to express the different Cya reporter constructs. Mean and SD are shown for one representative out of three independent replica experiments.

(C) Steady-state FLAG-Cya fusion protein levels of the indicated *Bh* strains grown on IPTG-containing medium.

doi:10.1371/journal.ppat.0020115.g002

(pFLAG-Cya–*Bh* $BepD_{352–534}$). To test for translocation of *Bh* BepA, either full-length protein (*Bh* $BepA_{1–544}$) or the C-terminal domain harboring the putative T4S signal (*Bh* $BepA_{305–544}$) was fused to FLAG-Cya. These reporter constructs were expressed either in *Bh* wild-type or in the *ΔvirB4* mutant lacking a functional VirB/VirD4 system. HUVECs infected with wild-type-expressing FLAG-Cya did not display any significant increase of the cAMP level compared with wild-type without the pFLAG-Cya plasmid. In contrast, FLAG-Cya fused to either *Bh* $BepD_{352–534}$, *Bh* $BepA_{1–544}$, or *Bh* $BepA_{305–544}$ resulted in an approximately 10-fold increase of intracellular cAMP levels in HUVECs (Figure 2B). This effect was dependent on a functional VirB/VirD4 system. In summary, we show that BepA is a VirB/VirD4 substrate that harbors a functional C-terminal T4S signal.

The BID Domain of *Bh* BepA Is Sufficient to Inhibit Apoptosis

Next, we determined whether ectopic expression of *Bh* BepA in HUVECs is sufficient to mediate anti-apoptosis. N-terminal green fluorescent protein (GFP) fusions to full-length *Bh* BepA or fragments thereof were constructed in an appropriate eukaryotic expression vector. As control we included the expression vector pGFP encoding just GFP (Figure 3A). Then, 24 h after transfection of HUVECs with the different GFP fusion constructs, cells were either exposed to actinomycin D (apoptosis induction) or left untreated (non-induced control) for another 12 h. Then, cells were stained with Annexin V and PI, and the proportion of apoptotic cells among the GFP-positive cell population was quantified by flow cytometry.

HUVECs transfected with pGFP and treated with actinomycin D displayed an apoptotic rate of 13% (Figure 3B). Fusion of full-length *Bh* BepA to the C-terminus of GFP (pGFP–*Bh* $BepA_{1–544}$) reduced the apoptotic population almost 4-fold to a level similar to that of the non-induced control. The same anti-apoptotic activity was observed when only the C-terminal bipartite T4S signal of *Bh* BepA was fused, thus missing the first 304 N-terminal amino acids encoding the FIC domain (pGFP–*Bh* $BepA_{305–544}$). In contrast, fusion of the FIC domain (pGFP–*Bh* $BepA_{1–304}$) did not result in inhibition of apoptosis. Further analysis showed that fusion of the BID domain (142 amino acids [aa]) to GFP (pGFP–*Bh* $BepA_{305–446}$) was sufficient to inhibit apoptosis, whereas fusion of the positively charged C-terminal tail plus only part of the BID domain (pGFP–*Bh* $BepA_{403–544}$) did not result in anti-apoptosis (Figure 3B). Rather, expression of the latter construct had a pro-apoptotic effect, as indicated by

the increased apoptotic cell population in the untreated sample. Taken together, these data demonstrate that ectopic expression of the BID domain as part of the bipartite T4S signal of *Bh* BepA in ECs is sufficient to mediate protection against apoptosis.

Anti-Apoptotic *Bh* BepA Constructs Associate with the Plasma Membrane

To test for the subcellular localization of *Bh* BepA in host cells, the generated GFP fusions (Figure 3A) were ectopically expressed in HEK293T cells for 24 h, followed by immunocytochemical staining for the cell surface with Texas Red–conjugated wheat germ agglutinin (WGA). Samples were analyzed by confocal microscopy by taking images in the *xy*-plane. To better distinguish between cytoplasmic and membrane-associated localization, we also captured images in an *xz*-plane (indicated in Figure 3C by dashed lines). Ectopically expressed GFP localized to the cytoplasm of HEK293T cells, whereas the GFP–*Bh* $BepA_{1–544}$ fusion localized to the plasma membrane (Figure 3C). Interestingly, all fusion proteins with anti-apoptotic activity localized to the plasma membrane, while those that did not confer protection localized primarily to the cytoplasm.

Fractionation of post-nuclear extracts of the transfected HEK293T cells by ultracentrifugation was used as an independent biochemical assay for analyzing the membrane or cytosolic localization of ectopically expressed GFP-BepA fusions. The obtained data (Figure 3D) were in good agreement with the microscopic analysis presented in Figure 3C, except that construct pGFP–Bh $BepA_{403–544}$ displayed both cytosolic and membrane localization.

Taken together, these data suggest that association with the plasma membrane is critical for the anti-apoptotic activity of *Bh* BepA.

Only BepA Orthologs from Vasoproliferative *Bartonella* Species Display Anti-Apoptotic Activity

To assess whether anti-apoptosis is a general feature of BepA homologs, we tested the orthologs encoded by other *Bartonella* species for this activity. *Bq* was previously shown to cause vascular tumor formation, whereas *Bt* was never associated with vascular lesions [9]. Consistent with these observations, only *Bh* and *Bq,* but not *Bt* wild-type, were able to block actinomycin D–triggered caspase-3/-7 activation in a T4S-dependent manner (Figure 4A). In the genome sequence of *Bq,* the *bepA* gene is annotated as a pseudogene [21]. Closer inspection of the sequence revealed that because of an internal stop codon and a downstream-located start codon in frame, this *bepA* locus is split into two open reading frames *(Bq bepA1* and *Bq bepA2). Bq bepA1* encodes a FIC domain, and *Bq bepA2* encodes a BID domain and the positively charged C-terminal tail, the latter representing a putative T4S signal. Comparison of the amino acid sequences of *Bq* BepA1 and *Bq* BepA2 with *Bh* BepA revealed high similarity (59% and 63%, respectively). We cloned *Bt bepA* and *Bq bepA2* into expression plasmids, which were introduced into *ΔbepA–G* (Figure 4B). As controls we included the paralogs *Bh bepB* and *Bh bepC,* which in the initial screening of *Bh* Beps were found to lack anti-apoptotic activity (Figure 4B and unpublished data). HUVECs were infected for 24 h with the different isogenic strains, and subsequently apoptosis was induced by actinomycin D. Of the tested BepA homologs, only *Bh* BepA and *Bq* BepA2 inhibited actinomycin D–triggered caspase-3/-7 activation (Figure 4C). These findings revealed that *Bq bepA2* encodes an anti-apoptotic effector. To assign *Bq* BepA2 as a novel T4S substrate, we translocated a FLAG-Cya-BepA2 fusion from *Bh* into HUVECs by the Cya reporter assay (unpublished data). These results show that the anti-apoptotic activity of BepA is conserved among two human pathogens with vasoproliferative capacity *(Bh* and *Bq),* but not in *Bt,* which has not been associated with vasoproliferation. Moreover, these data confirm the localization of the anti-apoptotic activity to the C-terminal region of BepA that composes a functional T4S signal [13].

Inhibition of Apoptosis Correlates with an Increased Intracellular cAMP Level

To identify potential survival pathways mediated by anti-apoptotic BepA, we analyzed Affymetrix GeneChip data obtained for the transcriptome of HUVECs infected with *Bh* wild-type versus the Δ*virB4* mutant impaired in T4S (M. Dehio, M. Schmid, M. Quebatte, and C. Dehio, unpublished data). These data revealed a T4S-dependent upregulation of the NFκB- and cAMP-dependent CREM/CREB regulons in HUVECs. Both signaling pathways have been described to mediate, among other functions, protection against apoptosis [22–24].

We tested whether these pathways were activated by anti-apoptotic BepA homologs. We monitored activation of the NFκB pathway in infected HUVECs by measuring the release of interleukin 8 (IL-8). *Bh* wild-type triggered an increased IL-8 release compared with Δ*bepA–G* or the uninfected control. In contrast, none of the BepA homologs expressed in Δ*bepA–G* induced increased IL-8 secretion (Figure 5A). This finding indicates that the survival mechanism triggered by anti-apoptotic BepA homologs is independent from the activation of the NFκB pathway triggered by wild-type bacteria. Activation of the cAMP-dependent CREM/CREB pathway was assayed by quantitative real-time PCR of two cAMP-inducible genes, namely *pde4B* and *crem* [25,26]. Only strains translocating anti-apoptotic BepA homologs were found to induce the expression of these genes in a statistically significant manner (Figure 5B). By quantifying intracellular cAMP upon infection of HUVECs by the various isogenic *Bh* strains, we further demonstrated that anti-apoptotic BepA homologs significantly increase the intracellular cAMP level (Figure 5C).

A Rise in Intracellular cAMP Results in Protection of ECs against Apoptosis

Since translocation of anti-apoptotic BepA homologs resulted in a rise of the intracellular cAMP level, we further studied the role of cAMP in anti-apoptosis. The intracellular cAMP level is regulated by adenylate cyclases (ACs) generating cAMP, and phosphodiesterases degrading cAMP [27,28]. To trigger a physiological rise of the cAMP level in ECs, we activated ACs with forskolin and in parallel inhibited cAMP degradation by adding the phosphodiesterase-inhibiting drug 3-isobityl-1-methylxanthine (IBMX) [29,30]. HUVECs were infected with the substrate-free Δ*bepA–G* strain and with the BepA-expressing strain Δ*bepA–G*/p*Bh* BepA in the absence and presence of forskolin/IBMX. Apoptosis was induced by exposure to actinomycin D and monitored by measuring caspase-3/-7 activity. By adding forskolin/IBMX we were able

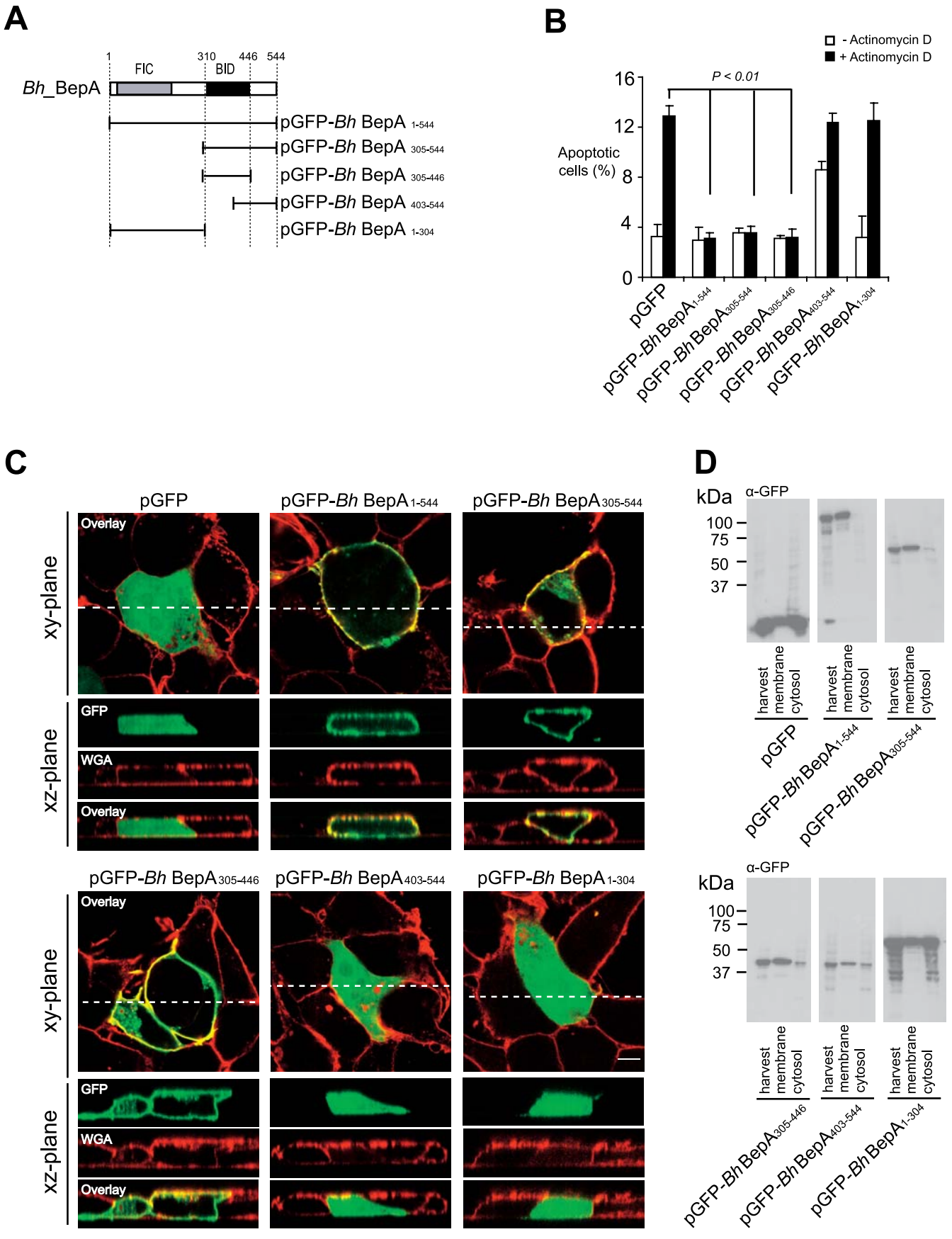
A
1
310
446
544
FIC
BID
Bh_BepA
pGFP-Bh BepA 1-544
pGFP-Bh BepA 305-544
pGFP-Bh BepA 305-446
pGFP-Bh BepA 403-544
pGFP-Bh BepA 1-304
B
- Actinomycin D
+ Actinomycin D
P < 0.01
Apoptotic cells (%)
16
12
8
4
0
pGFP
pGFP-BhBepA1-544
pGFP-BhBepA305-544
pGFP-BhBepA305-446
pGFP-BhBepA403-544
pGFP-BhBepA1-304
C
pGFP
pGFP-Bh BepA1-544
pGFP-Bh BepA305-544
pGFP-Bh BepA305-446
pGFP-Bh BepA403-544
pGFP-Bh BepA1-304
xy-plane
xz-plane
Overlay
GFP
WGA
D
kDa
α-GFP
100
75
50
37
harvest
membrane
cytosol
pGFP
pGFP-BhBepA1-544
pGFP-BhBepA305-544
pGFP-BhBepA305-446
pGFP-BhBepA403-544
pGFP-BhBepA1-304

Figure 3. Delineation and Subcellular Localization of the Region of *Bh* BepA Required for Inhibition of Apoptosis

(A) Schematic presentation of N-terminal GFP fusions to parts of *Bh* BepA.

(B) Determination of apoptosis following ectopic expression of the constructs illustrated in (A). GFP-BepA fusion proteins were ectopically expressed in HUVECs for 24 h, followed by 12 h incubation in the presence or absence of actinomycin D as indicated. The loss of membrane asymmetry in transfected cells (GFP-positive) was then quantified by flow cytometric analysis of APC-Annexin V– and PI-stained cells, allowing us to quantify the rate of apoptotic cells (Annexin V–positive and PI-negative). The means and SD of three independent replica experiments are shown. The *p*-values were determined by using an unpaired Student's *t*-test.

(C) The GFP–*Bh* BepA fusion proteins illustrated in (A) were ectopically expressed for 24 h in HEK293T cells. Cells were immunochemically stained to label the cell surface with Texas Red–conjugated WGA. Confocal pictures were taken for GFP (green channel) and WGA (red channel) in the *xy*-plane (upper image, overlay both channels, bar = 10 μm), and also in the *xz*-plane at the dashed stroke line (lower images, single channels and overlay channels).

(D) Fractionation of GFP–*Bh* BepA fusion proteins into membrane and cytosolic fractions by ultracentrifugation of post-nuclear extracts harvested from transfected HEK293T cells.

doi:10.1371/journal.ppat.0020115.g003

to reduce caspase-3/-7 activity in uninfected HUVECs and cells infected with the Δ*bepA–G* strain to a level similar to that found in cells infected with Δ*bepA*–G/p*Bh* BepA. Interestingly, the addition of forskolin/IBMX did not have an additive protection effect in Δ*bepA–G*/p*Bh* BepA–infected HUVECs (Figure 6A). The same results were obtained by adding the cell-permeable cAMP analog dibutyryl cAMP to the culture medium (Figure 6B). From these data we conclude that a moderately increased intracellular cAMP level, as triggered by *Bh* BepA, is sufficient to protect ECs against apoptosis.

The Role of *Bh* BepA in Evading CTL-Mediated Apoptosis

During colonization of the human endothelium, intracellular *Bh* are hidden from antibody- and complement-mediated immune responses [9]. However, the infected ECs may be killed by CTLs [31]. To study a putative role of *Bh* BepA in protecting ECs from CTL-mediated apoptosis, we used a major histocompatibility complex (MHC) class I–restricted CTL clone that kills HLA-A2-positive HUVECs upon extracellular loading with a Y-chromosome-encoded, male-specific minor histocompatibility Ag peptide with the sequence FIDSYICQV (SMCY peptide) [32]. To specifically measure the rate of EC apoptosis without interference by apoptotic CTLs, we pre-labeled the EC population with the fluorogenic dye CSFE. Pre-labeled HUVECs were left uninfected (control), or infected with wild-type, Δ*bepA–G*, or Δ*bepA–G*/p*Bh* BepA. Then, 24 h after infection, HUVECs were either pre-loaded for 30 min with the CTL-stimulating SMCY peptide (10^{-5} M) or not pre-loaded. After washing, CTLs were added in an effector-to-target cell ratio of 5:1. At different time points (0 h, 2.5 h, and 6 h), Annexin V and PI staining was performed to quantify the amount of apoptotic HUVECs (CSFE-positive, Annexin V–positive, and PI-negative) (Figure 7A and 7B). SMCY-treated HUVECs, which were either uninfected or pre-infected with the BepA-deficient Δ*bepA*–G mutant strain, displayed a time-dependent increase in the apoptotic population in comparison with respective control cells without pre-loading of the CTL-activating SMCY peptide. In sharp contrast, SMCY-treated HUVECs pre-infected with wild-type or the BepA-expressing strain Δ*bepA–G*/p*Bh* BepA did not display any significant increase of apoptosis over control cells without pre-loading with the SMCY peptide. These data indicate that BepA is capable of protecting ECs against the MHC class I–restricted apoptotic activity of CTLs. Consistently, we noticed that BepA-expressing bacteria, as well as the ectopic expression of a GFP–*Bh* BepA fusion protein alone, protected ECs against cell death triggered by a different CTL clone, which was activated by phytohemagglutinin in an MHC class I–independent manner (unpublished data). Together, these data indicate that translocated *Bh* BepA can effectively protect the chronically infected vascular endothelium against CTL-mediated cell death.

Discussion

The modulation of host cell apoptosis is a recurrent theme in bacterial pathogenesis [1]. Research in this area focused initially on the pro-apoptotic mechanisms triggered by pathogens that typically cause acute infections (e.g., *Shigella, Salmonella,* and *Yersinia* species). Some pro-apoptotic effectors and their targeted cellular pathways have been studied in molecular detail [33,34]. More recently, pathogen-triggered anti-apoptosis was recognized as an important virulence trait of bacteria that predominately cause chronic infection (e.g., *Bartonella, Brucella, Chlamydia, Helicobacter, Mycobacterium,* and *Rickettsia* species) and thus need to protect their cellular habitats by suppressing host-triggered apoptosis [35]. However, the bacterial effectors, and to a large extent also the cellular pathways involved in mediating pathogen-induced anti-apoptosis, remain poorly defined. In the case of *Bh* and *Bq,* the formation of vascular tumors in immunocompromised patients was shown to be linked to the inhibition of apoptosis of infected ECs [10]. In this report, we identified the anti-apoptotic factor of these vasoproliferative bartonellae. Deletion of the *Bh bepA* gene resulted in the complete loss of the anti-apoptotic activity of *Bh,* whereas expression of *Bh bepA* in *trans* restored the activity to wild-type level. *Bh* BepA was previously described as a putative substrate of the T4S system VirB/VirD4 [13]; we used the Cya reporter assay to demonstrate that *Bh* BepA is indeed translocated into ECs in a T4S-dependent manner. *Bh* BepA is thus a genuine T4S effector that inhibits apoptosis upon translocation into HUVECs. It is worth noting that we have been unable to show translocation of *Bh* BepA by CRAfT, an assay that we previously used to demonstrate translocation of several other *Bh* Beps [13]. Nuclear import of the Cre reporter protein fusion is a prerequisite for a positive readout by CRAfT [13], suggesting that the negative readout obtained for *Bh* BepA fusions could result from protein recruitment to an intracellular localization that interferes with nuclear import. Indeed, ectopic expression of full-length *Bh* BepA fused to GFP revealed a prominent localization of the fusion protein to the plasma membrane, in contrast to the cytosolic localization of GFP alone. Unlike ectopically expressed GFP, the GFP–*Bh* BepA fusion also conferred protection against EC apoptosis. These data demonstrate that *Bh* BepA is not only required but also sufficient for inhibiting EC apoptosis,

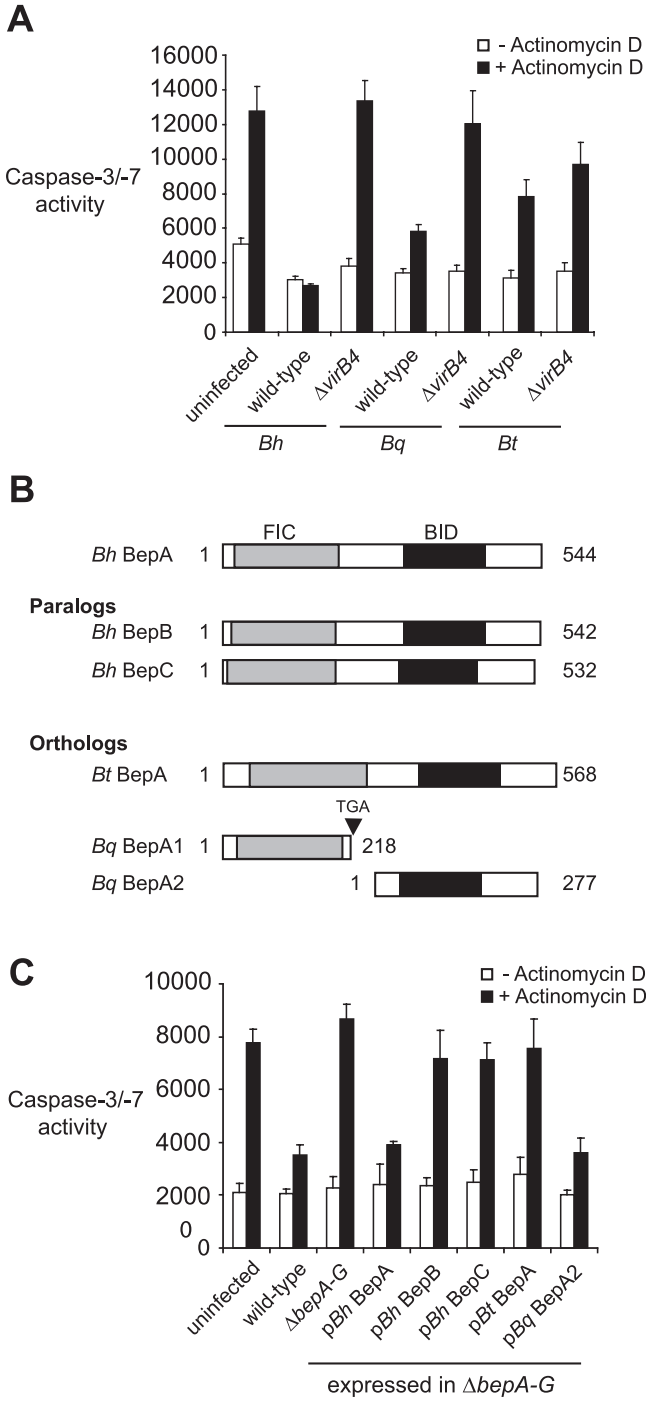

Figure 4. Comparison of the Anti-Apoptotic Activities of BepA Homologs

(A) Anti-apoptotic activities of wild-type and isogenic Δ*virB4* mutant strains of *Bh* in comparison with *Bq* and *Bt*.

(B) Domain structure of *Bh* BepA, its paralogs *Bh* BepB and *Bh* BepC, and the orthologs *Bt* BepA and *Bq* BepA1/*Bq* BepA2. These homologs contain conserved FIC and BID domains in their N-terminal and C-terminal regions, respectively, except for *Bq*, where the orthologous locus is split between these domains into two separate open reading frames by an internal stop codon.

(C) Anti-apoptotic activity of BepA homologs. HUVECs were infected with the indicated *Bh* strains for 24 h, followed by apoptotic induction with actinomycin D for 12 h. Caspase-3/-7 activities were then determined with a specific fluorogenic peptide substrate. Mean and SD are illustrated for one representative out of three independent experiments.

doi:10.1371/journal.ppat.0020115.g004

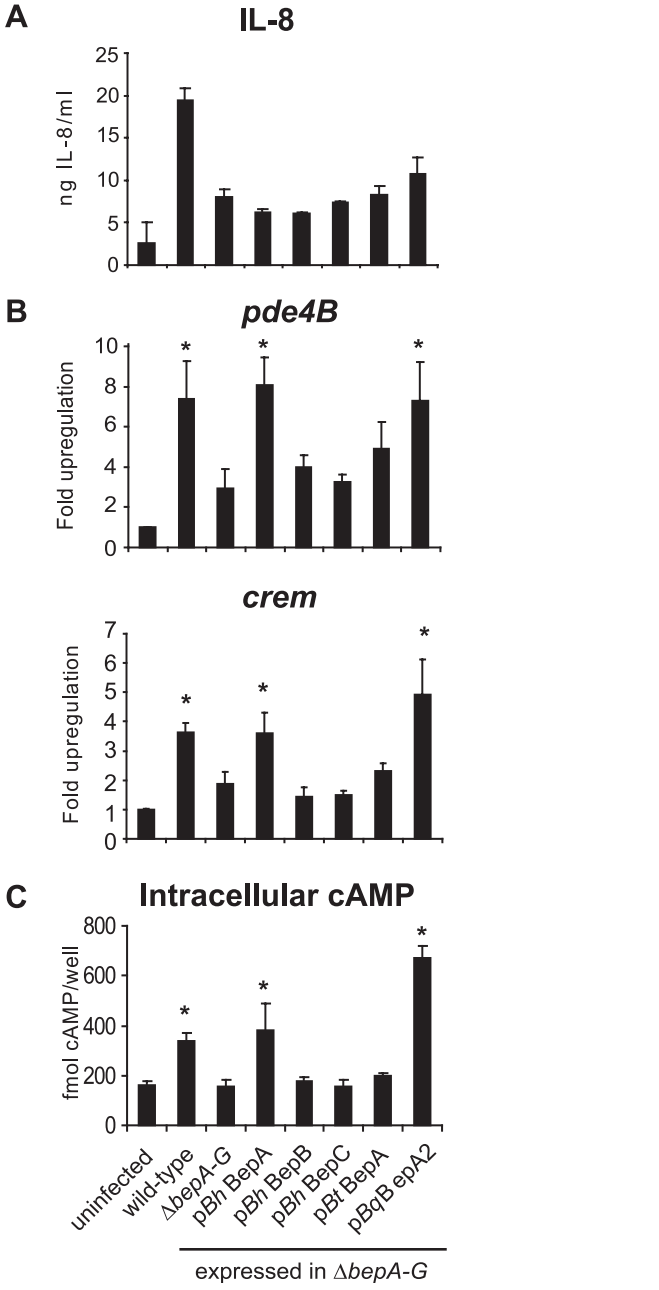

Figure 5. Anti-Apoptotic BepA Homologs Mediate an Increase in Intracellular cAMP and an Upregulation of cAMP Response Genes

HUVECs were infected with the indicated *Bh* strains. The means and SD of one out of three independent replica experiments performed in triplicate samples are presented.

(A) IL-8 was determined in culture supernatants after infection for 54 h with MOI = 300.

(B) Expression of the cAMP-responsive genes *pde4B* and *crem* was determined by quantitative real-time PCR after infection for 54 h with MOI = 300.

(C) Intracellular cAMP levels were determined after infection for 30 h with MOI = 150.

In (B) and (C), samples marked with an asterisk ($p < 0.05$) differ statistically significantly from Δ*bepA–G* using an unpaired Student's *t*-test.

doi:10.1371/journal.ppat.0020115.g005

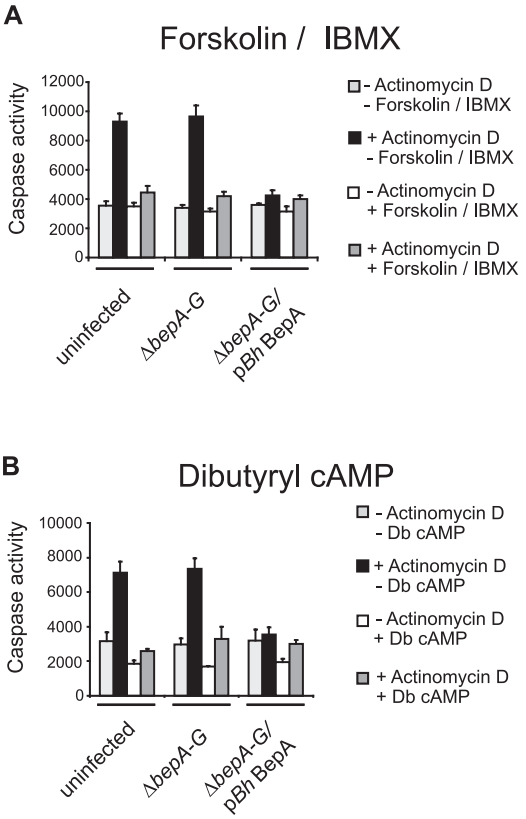

Figure 6. A Pharmacologically Increased cAMP Level in ECs Mimics the Anti-Apoptotic Effect of *Bh* BepA

HUVECs were infected for 24 h with the indicated *Bh* strains or left uninfected (control) in the absence or presence of either (A) forskolin (1 μM) and IBMX (10 μM) or (B) dibutyryl cAMP (1 mM). If indicated, apoptosis was then induced with actinomycin D. Caspase-3/-7 activities were determined 9 h later. All strains were tested in triplicates a minimum of three times.

doi:10.1371/journal.ppat.0020115.g006

and that this anti-apoptotic effector localizes to the plasma membrane. Moreover, ectopic expression of various parts of *Bh* BepA fused to GFP revealed a strict correlation of the capacity to mediate anti-apoptosis with localization to the plasma membrane (as opposed to the primarily cytoplasmic localization of fusions that did not cause anti-apoptosis). This finding indicates that plasma membrane targeting may be important for the anti-apoptotic activity of *Bh* BepA.

In search of the cellular pathway by which *Bh* BepA mediates anti-apoptosis in ECs, we first tested whether an NFκB-dependent survival pathway is involved. The anti-apoptotic activity of *R. rickettsii* in ECs was reported to depend on NFκB activation [5], and we have previously shown that *Bh* activates NFκB in a VirB/VirD4- and Bep-dependent manner [13]. Here, we demonstrated that *Bh* BepA alone does not trigger the NFκB-dependent secretion of IL-8; even so, it fully protects against apoptosis. Thus, NFκB does not seem critical for *Bh* BepA–mediated anti-apoptosis. Affymetrix GeneChip experiments indicated that *Bh* also triggers a cAMP signaling pathway in a T4S-dependent manner (M. Dehio, M. Schmid, M. Quebatte, and C. Dehio, unpublished data). Here, we have shown that the anti-apoptotic activity of *Bh* BepA in HUVECs correlates with elevation of the intracellular cAMP level and results in the upregulation of cAMP-stimulated gene expression. Recently, it emerged that the regulation of apoptosis is an important facet of cAMP signal transduction [30,36–38]. Moderately elevated cAMP levels were reported to protect several cell types against apoptosis, while the survival mechanisms differed from cell type to cell type and were considered to require the activation of protein kinase A, extracellular signal regulated, mitogen-activated protein kinase, or guanine nucleotide exchange factor signaling pathways, which subsequently resulted in the expression of anti-apoptotic genes [23,36,37,39–44]. In our system, the specific downstream signaling pathway mediating cAMP-dependent anti-apoptotis remains elusive: efforts to block putatively involved signaling molecules (i.e., protein kinase A) failed because of apparent cytotoxic effects of effective inhibitor concentrations during the extended time frame of the apoptosis assay.

Importantly, a physiological rise in the intracellular cAMP level has been reported to fully protect ECs against apoptosis [45]. Consistent with this, we observed that increased cAMP levels caused by the combined action of the AC-activating drug forskolin and the phosphodiesterase-inhibiting drug IBMX resulted in a complete suppression of actinomycin D–induced apoptosis in HUVECs. Forskolin/IBMX-treated cells displayed an increase in the expression of cAMP-regulated genes similar to that observed upon infection with anti-apoptotic *Bh* strains. cAMP is produced in eukaryotic cells by the family of membrane-anchored ACs. ACs are activated by heterotrimeric G proteins that are regulated by G protein–coupled receptors [46]. Since the anti-apoptotic activity of *Bh* BepA in HUVECs is strictly associated with the plasma membrane localization of this effector, concomitant with an increase in the cAMP level, we propose that *Bh* BepA may trigger anti-apoptosis by interacting either with ACs directly, or with plasma membrane–associated heterotrimeric G proteins or G protein–coupled receptors that regulate AC activity.

Ectopic expression of GFP fusions with different parts of *Bh* BepA confined the anti-apoptotic activity to a region of 142 aa, which corresponds to the BID domain. This conserved domain was previously shown to be present in a least one copy in all Beps of *Bh* and *Bq* [13,14,21]. The BID domain plus the C-terminal positively charged tail sequence of the Beps was shown to constitute a bipartite translocation signal for T4S [13]. Interestingly, in contrast to the BID domain of *Bh* BepA, the conserved BID domains of the paralogs *Bh* BepB and *Bh* BepC have not been associated with anti-apoptosis. This indicates that subsequent to the expansion of this paralogous protein family by gene duplication, the *Bh* BepA BID domain acquired, in addition to its crucial function as a signal for T4S, the capacity to mediate anti-apoptosis. How this rather short domain may mediate these unrelated activities is presently unknown. It may be speculated that the BID domain represents a basic fold that mediates a protein–protein interaction with the T4S machinery that is crucial for protein translocation, and that in *Bh* BepA this basic fold is adapted to also mediate specific interaction with the plasma membrane–associated, cAMP-generating signaling cascade of ECs.

Each of the paralogs *Bh* BepA, *Bh* BepB, and *Bh* BepC carries in the N-terminal region one copy of the FIC domain. While this conserved domain of unknown function might be

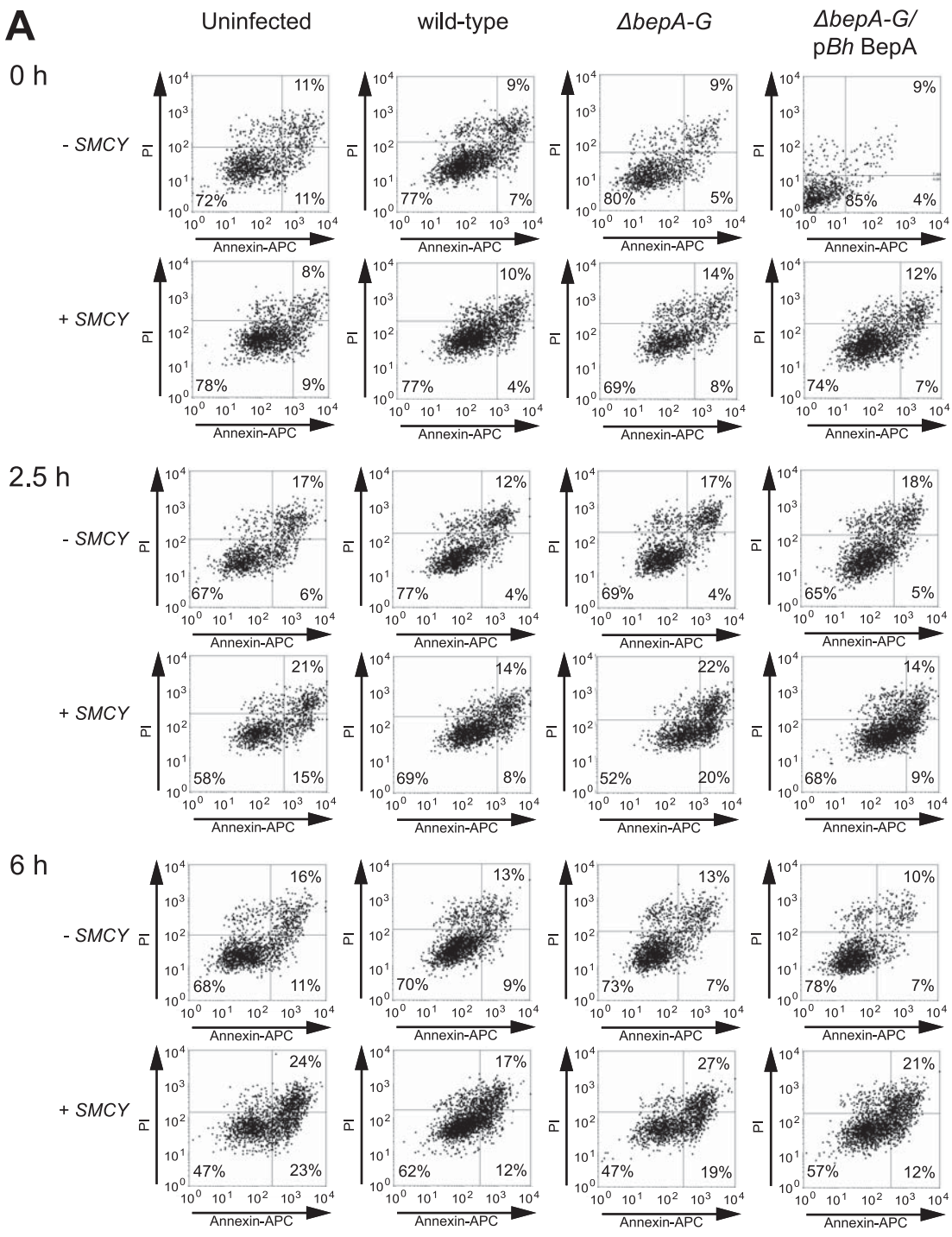
A
Uninfected
wild-type
ΔbepA-G
ΔbepA-G/ pBh BepA
0 h
- SMCY
+ SMCY
2.5 h
6 h
PI
Annexin-APC
11%
72%
11%
9%
77%
7%
9%
80%
5%
9%
85%
4%
8%
78%
9%
10%
77%
4%
14%
69%
8%
12%
74%
7%
17%
67%
6%
12%
77%
4%
17%
69%
4%
18%
65%
5%
21%
58%
15%
14%
69%
8%
22%
52%
20%
14%
68%
9%
16%
68%
11%
13%
70%
9%
13%
73%
7%
10%
78%
7%
24%
47%
23%
17%
62%
12%
27%
47%
19%
21%
57%
12%

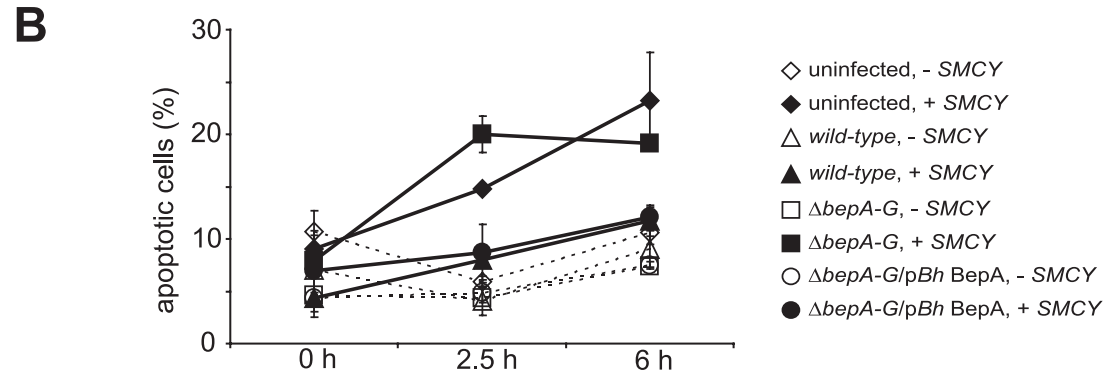
B
apoptotic cells (%)
30
20
10
0
0 h
2.5 h
6 h
uninfected, - SMCY
uninfected, + SMCY
wild-type, - SMCY
wild-type, + SMCY
ΔbepA-G, - SMCY
ΔbepA-G, + SMCY
ΔbepA-G/pBh BepA, - SMCY
ΔbepA-G/pBh BepA, + SMCY

Figure 7. *Bh* BepA Protects ECs against CTL-Mediated Cell Death

Confluent HUVEC monolayers fluorescently labeled with the cell-tracking dye CFSE were infected with the indicated bacterial strains for 24 h or left uninfected (control). Then cells were incubated in the presence (+ SMCY) or absence (− SMCY) of SMCY peptides, followed by washing. CTLs were added in an effector-to-target cell ratio of 5:1 for the indicated period, and after washing and Annexin V– and PI-staining, the apoptotic cell population of HUVECs was determined by flow cytometry analysis (CFSE-positive, Annexin V–positive, and PI-negative).

(A) Dot plots are shown for representative samples.

(B) Summary graph representing HUVEC apoptosis during CTL co-culture. The mean and SD of one of two independent experiments performed in duplicates is shown.

doi:10.1371/journal.ppat.0020115.g007

important for the effector function of *Bh* BepB and *Bh* BepC, our results demonstrate that the FIC domain is dispensable for the anti-apoptotic activity of *Bh* BepA. Interestingly, an internal stop codon and downstream-located start codon within the *bepA* ortholog of *Bq* split this locus into two separate open reading frames *(Bq bepA1* and *Bq bepA2). Bq* BepA1 has the FIC domain but lacks a T4S signal, and thus cannot be translocated into ECs. In contrast, *Bq* BepA2 consists only of the T4S signal, which we have shown mediates both T4S-dependent translocation and anti-apoptosis in ECs. It thus appears plausible that the functional diversification of BepA into an anti-apoptotic effector occurred in the common ancestor of the closely related species *Bh* and *Bq* [21], and that following speciation the acquisition of additional mutations resulted in the elimination of the dispensable N-terminal FIC domain in *Bq*.

Interestingly, unlike *Bh* BepA and *Bq* BepA2, the BepA ortholog of *Bt* does not mediate any anti-apoptotic activity, nor any measurable activation of the cAMP pathway. This observation is in agreement with the previously reported finding that, among the bartonellae, the anti-apoptotic activity is limited to the vasoproliferative species *Bh* and *Bq* [10].

To asses if the here identified anti-apoptotic activity of *Bh* BepA might be able to protect the cellular habitat of *Bh* during the infection process, we used a co-culture system of HUVECs with human CTLs. CTLs execute cell-mediated immunity, an immune mechanism probably involved in the elimination of *Bh* infection [9,12,47]. Cell-mediated immunity particularly serves as a defense mechanism against microbes that survive and replicate inside infected host cells. Upon recognition of MHC class I–displaying microbial peptides, CTLs are activated to kill their target cells by the release of perforin and granzymes [31,48]. Perforin forms pores in the target cell membrane and assists the delivery of pan-caspase-activating granzymes into the cytoplasm of the target cell [44,49,50]. In our study, we used a CTL clone that is activated in an MHC class I–restricted manner by extracellular loading of HLA-A2-positive HUVECs with an HLA-A2-specific peptide (SMCY). Such activated CTLs kill their target cells in a perforin-dependent manner [32], primarily by triggering granzyme-dependent apoptosis [50,51]. *Bh* BepA–expressing strains indeed inhibited CTL-triggered EC apoptosis, indicating that the biological function of *Bh* BepA expression in vivo might be to protect the integrity of its colonized cellular niche. The *Bh* BepA–mediated resistance of ECs to CTL-dependent cell death points towards an important role of BepA in escaping cell-mediated immunity and thus in protecting the integrity of the chronically infected vasculature, which is a prerequisite for vascular proliferation. The establishment of an animal model for *Bartonella*-triggered vasoproliferation now appears an urgent need for studying the precise contribution of BepA-mediated anti-apoptosis in the process of vascular tumor formation.

In summary, the anti-apoptotic T4S effectors *Bh* BepA and *Bq* BepA2 characterized in this study represent striking examples of the evolution of new pathogenic traits in bacteria. The delineation of their anti-apoptotic activity to the conserved BID domain, and their proposed role in maintaining the cellular habitat by mediating anti-apoptosis via specific interaction with the plasma membrane–associated, cAMP-generating signaling cascade of ECs, should pave the way for future studies to elucidate the molecular and structural basis of *Bartonella*-mediated anti-apoptosis in the vascular endothelium and the role of this pathological process in vasoproliferative tumor growth.

Materials and Methods

Bacterial strains and growth conditions. The bacterial strains used in this study are listed in Table 1. *Bartonella* spp. were grown on Columbia agar plates containing 5% defibrinated sheep blood (CBA plates) at 35 °C and 5% CO_2 for 2–4 d. Strain RSE247, a spontaneous streptomycin-resistant strain of *Bh* ATCC 49882^T [12], served as wild-type in this study. When indicated, media were supplemented with 30 μg/ml kanamycin, 100 μg/ml streptomycin, 12.5 μg/ml gentamicin, and/or 500 μM isopropyl β-D-thiogalactosidase (IPTG). *Escherichia coli* strains were cultivated in Luria-Bertani liquid medium, or after addition of agar on plates, at 37 °C overnight. When indicated, media were supplemented with 50 μg/ml kanamycin, 200 μg/ml ampicillin, 25 μg/ml gentamicin, 500 μM IPTG, and/or 1 mM diaminopimelic acid.

DNA manipulation. Plasmids used in this study are listed in Table 1. Primers are listed in Table 2.

Plasmids for in-frame deletions and complementation of deletion mutants were constructed as follows: pMS5 used for creating the Δ*bepA* mutant was already described before [13]. The use of pMS5 for gene replacement in RSE247 resulted in the Δ*bepA* mutant MSE154. Plasmid pRS63, used for generating a Δ*virB4* in-frame deletion mutant in *Bq,* was constructed as follows. The BamHI insert of pRS14 [16] was replaced by a 1,318-bp BamHI fragment of the *Bq virB* locus containing a 2,112-bp in-frame deletion in *virB4*. This fragment was constructed by megaprime PCR from two PCR products. Product 1 (0.75 kb) was amplified with primers prRS226 and prRS227 and contained the first 115 bp of the *virB4* gene and upstream sequences. Product 2 (0.55 kb) was amplified with primers prRS228 and prRS229 and contained the last 120 bp of the *virB4* gene and downstream sequences. Megapriming and PCR amplification with primers prRS226 and prRS229 were performed as described [16].

Plasmids for complementation of *ΔbepA* mutant and *ΔbepA–G* mutant were constructed as follows: For constructing vectors expressing N-terminal FLAG-tagged Bep proteins, the plasmid pPG100 was used. The fragments were generated by PCR amplification from chromosomal DNA of RSE247 and *Bt,* using oligonucleotide primers prPG92/93, prPG95/129, prPG97/130, or pMS27/28, and were inserted by the flanking NdeI site into the corresponding site of pPG100, resulting in pPG101 (encoding *Bh* BepA), pMS006 (encoding *Bh* BepB), pMS007 (encoding *Bh* BepC), and pMS011 (encoding *Bt* BepA). To construct plasmid pMS100, carrying a multiple cloning site, prGS01 and prGS02 were annealed together and the resulting 45-bp fragment was inserted into pPG100 using the NdeI site. Using oligonucleotide primers pMS102 and prMS103, a fragment of 0.85 kb was amplified using chromosomal DNA of *Bq* as template. Then, using SalI/XmaI sites, this fragment was inserted into the corresponding site of pMS100, giving rise to pMS106. Plasmid pMS105 was constructed as follows: using flanking SalI/XmaI sites, the 1.65-kb PCR fragment

Table 1. Bacterial Strains and Plasmids Used in This Study

Strain or Plasmid	Name	Genotype or Relevant Characteristics	Reference or Source
***Bh* strains**	ATCC 49882^T	Houston-1, isolated from a bacteremic HIV patient	[57]
	MSE150	Δ*bepA–G* mutant of RSE247	[13]
	MSE154	Δ*bepA* mutant of RSE247	This work
	MSE156	MSE150 containing pPG101	This work
	MSE159	MSE150 containing pMS007	This work
	MSE162	MSE150 containing pRS51	[13]
	MSE164	MSE154 containing pRS51	This work
	MSE166	MSE154 containing pPG101	This work
	MSE167	MSE150 containing pMS006	This work
	MSE175	MSE150 containing pMS011	This work
	MSE218	MSE150 containing pMS100-A	This work
	MSE220	MSE150 containing pMS100-D	This work
	MSE226	MSE150 containing pMS100-B	This work
	MSE228	MSE150 containing pMS100-C	This work
	MSE240	MSE150 containing pMS102	This work
	MSE242	MSE150 containing pMS104	This work
	MSE249	RSE247 containing pMS400	This work
	MSE251	RSE247 containing pMS401	This work
	MSE253	RSE247 containing pMS404	This work
	MSE255	RSE242 containing pMS400	This work
	MSE257	RSE242 containing pMS401	This work
	MSE259	RSE242 containing pMS404	This work
	MSE269	MSE150 containing pMS106	This work
	MSE273	RSE247 containing pMS406	This work
	MSE275	RSE242 containing pMS406	This work
	MSE277	RSE247 containing pMS405	This work
	MSE279	RSE242 containing pMS405	This work
	RSE232	RSE242 containing pRS51	[13]
	RSE242	ΔvirB4 mutant of RSE247	[12]
	RSE247	Spontaneous Sm^r strain of ATCC 49882^T, serving as wild-type	[12]
	RSE308	RSE247 containing pRS51	[13]
***Bq* strains**	JK-31	Isolated from a bacteremic patient with bacillary angiomatosis	[58]
	RSE356	Spontaneous Sm^r strain of JK-31, serving as wild-type	This work
	RSE569	*ΔvirB4* mutant of RSE356	This work
	VR 358		[58]
***Bt* strains**	IBS 506^T	Isolated from a brown rat *(Rattus norvegicus)* (CIP 105476^T)	[16]
	RSE149	Spontaneous Sm^r strain of IBS 506T, serving as wild-type	[16]
	RSE173	*ΔvirB4* mutant of RSE149	[16]
***E. coli* strains**	β2150	*F′ lacZDM15 lacI^q traD36 proA+B+ thrB1004 pro thi strA hsdS lacZΔM15* Δ*dapA*::erm (Erm^R) pir	[16]
	NovaBlue	*endA1 hsdR17*(r K12–m K12+) *supE44 thi-1 recA1 gyrA96 relA1 lac*[*F′ proA+B+ lacI^{q}ZΔM15*::Tn*10* (Tc^R)]	Novagen, Madison
Plasmids	pPG100	*E. coli– Bartonella* spp. shuttle vector, encoding a short FLAG epitope	[13]
	pPG101	Derivative of pPG100, encoding FLAG::*Bh* BepA	This work
	pRS40	Cre vector encoding NLS::Cre	[13]
	pRS48	Cre vector containing NLS::Cre::*Bh* BepA (aa 305–544)	This work
	pRS49	Cre vector encoding NLS::Cre::*Bh* BepB (aa 303–542)	[13]
	pRS50	Cre vector encoding NLS::Cre::*Bh* BepC (aa 292–532)	[13]
	pRS51	Cre vector encoding NLS::Cre::*Bh* BepD (aa 352–534)	[13]
	pRS55	Cre vector encoding NLS::Cre::*Bt* BepA (aa 326–568)	This work
	pMS005	Mutagenesis vector for generating a *ΔbepA* in-frame deletion in *Bh*	[13]
	pMS006	Derivative of pPG100, encoding FLAG::*Bh* BepB	This work
	pMS007	Derivative of pPG100, encoding FLAG::*Bh* BepC	This work
	pMS013	Cre vector containing NLS::Cre::*Bh* BepA (aa 1–544)	This work
	pMS011	Derivate of pPG100, encoding FLAG::*Bt* BepA	This work
	pMS100	Insertion of a multiple cloning site into pPG100	This work
	pMS106	Derivate of pMS100, encoding FLAG::*Bq* BepA2	This work
	pMS100-A	Derivate of pMS100, encoding FLAG::*Bh* BepA (aa 305–542)	This work
	pMS100-B	Derivate of pMS100, encoding FLAG::*Bh* BepB (aa 303–542)	This work
	pMS100-C	Derivate of pMS100, encoding FLAG::*Bh* BepC (aa 292–542)	This work
	pMS100-D	Derivate of pMS100, encoding FLAG::*Bh* BepD (aa 352–534)	This work
	pMS105	Insertion of *Bh* BepA into pMS100	This work
	pMS111	Containing the hybrid *yopE-cyaA* gene	[19]
	pMS400	pMS100 containing a 1.23-kb PCR fragment carrying the *cya* of *Bordetella pertussis* (amplified from pMS111-Cornelis)	This work
	pMS401	Cya vector encoding *Bh* BepA (aa 305–542)	This work
	pMS404	Cya vector encoding *Bh* BepD (aa 252–534)	This work
	pMS405	Cya vector encoding *Bh* BepA	This work
	pMS406	Cya vector encoding *Bq* BepA2	This work

doi:10.1371/journal.ppat.0020115.t001

Table 2. Oligonucleotide Primers Used in This Study

Name	Sequence[a]	Restriction Site
prCREMfw	ATCGCCCGGAAGTTTGC	
prCREMrv	CAGCTCTCGTTTGCGTGTTG	
prGAPDHfw	GAAGGTGAAGGTCGGAGTC	
prGAPDHrv	GAAGATGGT GATGGGATTTC	
prGS001	TATGAAGGCCTCGAGTCGACCGCGGCCGCATCGATGACCCGGG (NdeI/StuI/XhoI/SalI/SacII/NotI/ClaI/XmaI)	
prGS002	TACCCGGGTCATCGATGCGGCCGCGGTCGACTCGAGGCCTTCA (XmaI/ClaI/NotI/SacII/SalI/XhoI/StuI/NdeI)	
prMS027	CGGGAATTCCATATGCAAAAGGGAATATTTCACT	NdeI
prMS028	CGGGAATTCCATATGTTAGCTGGCTATAGCGAGTA	NdeI
prMS037	ACGCGTCGACCTCCAAAGGCAAAAGCAAAAACG	SalI
prMS038	TCCCCCCGGGTTAGCTAGCCATGGCAAGC	XmaI
prMS068	TCCCCCCGGGATGCCAAAGGCAAAAGCAAAAA	XmaI
prMS069	CTAGTCTAGATTAGCTAGCCATGGCAAGC	XbaI
prMS074	TCCCCCCGGGAAGCATGTTGCACTCCTCA	XmaI
prMS075	CTAGTCTAGATTATTCGGCTTTTGGAGCTGTAA	XbaI
prMS076	TCCCCCCGGG GAGCTTGAAAACACGCTCAT	XmaI
prMS077	CTAGTCTAGATTAGCTGGCAATAGCAAGCG	XbaI
prMS078	GGAATTCCATATGCAGCAATCGCATCAGGCTG	NdeI
prMS083	TCCCCCCGGGGAATTAAAAAAAACACTCATCCC	XmaI
prMS084	CTAGTCTAGATTAACTTGGCATAGGGACCTCTT	XbaI
prMS090	TCCCCCCGGGTTACGAGGCCTGGCGTTCCACTGCGCCCA	XmaI/StuI
prMS102	ACGCGTCGACCGATGAGCCATATGAAAAATATCAAA	SalI
prMS103	TCCCCCCGGGTTAGCAAACTATTTTAGCTTGC	XmaI
prMS104	AGCTTTGTTTAAACGATGAGCCATATGAAAAATATCAAA	PmeI
prPG92	GGAATTCCATATGCCAAAGGCAAAAGCAAAAA	NdeI
prPG93	GGAATTCCATATGTTAGCTAGCCATGGCAAGC	NdeI
prPG095	GGAATTCCATATGTTAGCTGGCAATAGCAAGCG	NdeI
prPG097	GGAATTCCATATGTTAGTTGGTAAGAGCCCTTG	NdeI
prPG129	GGAATTCCATATGCCAAAAGCAAAAGCAAAAAA	NdeI
prPG130	GGAATTCCATATGTTAGAGCATAATTATCTGTA	NdeI
prRS167	TCCCCCCGGGTTAGCTAGCCATGGCAAGC	XmaI
prRS180	ATGGTGTCGAAAGAATTAAAAAAAACACTCATCC	SalI
prRS187	ATGGTGTCGACAAGAGTTAAAAAATATTCTCATTC	SalI
prRS188	TCCCCCCGGGTTAGCTGGCTATAGCGAGTA	XmaI

[a]Restriction endonuclease cleavage sites are underlined.
doi:10.1371/journal.ppat.0020115.t002

generated by prMS37/38 (chromosomal DNA of RSE247 serves as a template) was inserted into the corresponding sites in pRS40, yielding pMS13. Using flanking SalI/XmaI sites, the 1.65-kb fragment was shuttled into the SalI/XmaI sites of pMS100. Using oligonucleotide primers prRS167/180 and prRS187/188, fragments of 0.73-kb size were amplified using chromosomal DNA of RSE247 and of *Bt*, respectively, as template. Using flanking SalI/XmaI sites, the fragments were inserted into the corresponding site of pRS40, giving rise to pRS48 and RS55, respectively. C-terminal sequences of the different Bep proteins were shuttled into pMS100 using the flanking SalI/XmaI sites. The plasmids resulting from this step are given below, as well as the range of amino acids of a given Bep protein fused to the N-terminal FLAG: pMS100-A (shuttled from pRS48, aa 305–544 of *Bh* BepA), pMS100-B (shuttled from pRS49, aa 303–542 of *Bh* BepB), pMS100-C (shuttled from pRS50, aa 292–532), and pMS100-D (shuttled from pRS51, aa 352–534 of *Bh* BepD).

Plasmids for expression of Cya-Bep fusion proteins were constructed as follows: To construct pMS400, the *cya* of pMS111 was PCR-amplified with oligonucleotide primers prMS78/90 introducing a start and a stop codon to the resulting *cya* fragment. Using flanking NdeI/XmaI sites, the 1.23-kb fragment was inserted in the corresponding sites of pMS100. Plasmid pMS401 was derived by insertion of a 1.2-kb NdeI/StuI fragment of pMS400, which includes the *cya* gene without stop codon, into the corresponding sites of pMS100-A. The NdeI/StuI fragment of pMS400 was further inserted in the corresponding site of pMS100-D and pMS105, giving rise to pMS404 and pMS405, respectively. To construct pMS406, *Bq* BepA2 was PCR-amplified from chromosomal DNA of *Bq* with oligonucleotide primers prMS103/104. Using flanking PmeI/XmaI sites, the 0.86-kb fragment was inserted in the StuI/XmaI sites of pMS400.

Plasmids for ectopic expression of GFP-BepA fusion proteins were constructed as follows: To construct eGFP-Bep fusion proteins (see Figure 4A), pWAY21 (Molecular Motion Lab, http://momotion.cns.montana.edu), a CMV-driven EGFP for C-terminal fusion, was used as basic vector. The plasmids resulting from this step and the oligonucleotide primers used (with incorporated XmaI/XbaI sites used for cloning to the corresponding sites of pWAY21) are given below, as well as the range of amino acids of a given Bep protein fused to eGFP: pMS21 (primers prMS68/69, aa 1–544 of *Bh* BepA), pMS22 (primer prMS76/77, aa 302–542 of *Bh* BepB), pMS23 (primers prMS83/69, aa 305–544 of *Bh* BepA), pMS24 (primers prMS83/84, aa 305–446 of *Bh* BepA), pMS25 (primers prMS74/69, aa 403–544 of *Bh* BepA), pMS26 (primers prMS68/75, aa 1–304 of *Bh* BepA), and pMS27 (primers prMS105/106, aa 1–277 of *Bq* BepA2).

The integrity of all constructs was confirmed by sequence analysis and Western blotting using anti-FLAG M2 antibodies (Sigma-Aldrich, http://www.sigmaaldrich.com).

Generation of deletion mutants. pRS63 was used to generate the *ΔvirB4* mutant RSE569 in the RSE356 background as previously described for *Bt* [16]. The spontaneous streptomycin-resistant mutant RSE356 was obtained by selection of *B. quintana* JK-31 on 100 mg/l streptomycin.

Cell lines and cell culture. HUVECs were isolated as described [18]. HUVECs and the human embryonic kidney cell line HEK293T were cultured as described before [12]. The stable transfected endothelial cell line Ea.hy296/pRS56-c#B1 was cultured as reported [13].

Infection assay. HUVECs (passage 3–7) were plated as described before [12]. Unless stated differently, cells were infected with a multiplicity of infection (MOI) of 300 bacteria per cell [10] in M199/10% FCS/500 μM IPTG and incubated for the indicated time. If specified, 100 nM actinomycin D (Sigma-Aldrich) was added to trigger apoptosis as described before [10,12].

HUVEC transfection. HUVECs were transfected using Amaxa nucleofection technology (Amaxa, http://www.amaxa.com) following the manufacturer's guidelines for HUVEC transfection. After transfection, cells were seeded into 24-well plates or six-well plates.

HEK293T cell transfection. Subconfluent (2.5 million cells) HEK293T cells in 8-cm cell culture dishes were transfected with a total of 2.5 μg DNA following the protocol "Calcium phosphate–mediated transfection of eukaryotic cells with plasmid DNAs" [52]. After 12 h, the cell culture medium was replaced and the cells kept in culture for an additional 24 h before fixation for immunocytochemical staining or harvesting for subcellular localization of the transfected constructs.

Subcellular fractionation. Subcellular fractionation was performed according to standard protocols [53,54]. Briefly, confluent monolayers were washed three times with cold homogenization buffer (10 mM triethanolamine, 10 mM acetic acid, 1 mM EDTA, 250 mM sucrose [pH 7.4]), and cells were harvested by scraping and homogenized with a syringe and a 22-gauge 1/4 inch needle. The post-nuclear supernatant was obtained by centrifugation at 240*g* (15 min). Membranes were separated from cytosol by ultracentrifugation of the post-nuclear supernatant at 100,000*g* (30 min).

Caspase activity assay. The infection of HUVECs and the determination of caspase-3/-7 activity (MOI = 300) were carried out as described [12].

***cya* assay.** cAMP was assayed after 20 h contact between bacteria (MOI = 300) and HUVECs in 24-well plates. HUVECs were washed one time in pre-warmed PBS and lysed in denaturizing conditions as described previously [19]. cAMP was assayed by an EIA system (Biotrak; Amersham, http://www.amershambiosciences.com). Total cell proteins were assayed by the method of Bradford [55] (Bradford Reagent, Sigma-Aldrich).

CRAfT. The infection of the stably transfected Ea.hy926/pRS56-c#B1 cell line and the quantification of GFP-positive cells (percent positive events) by flow cytometry were carried out as described [13].

Immunoblot analysis. To monitor the steady-state level of Cya fusion proteins, bacteria were grown on IPTG-containing medium for 2 d. Cells were harvested and processed as described previously [13], except that anti-FLAG M2 (Sigma-Aldrich) was used as the primary antibody.

The stability of the different GFP fusion proteins used for ectopic expression in HUVECs was monitored after transient transfection of HEK293T cells. Cells were transfected by FuGENE 6 (Roche, http://www.roche.com) following the manufacturer's instructions. After 24 h expression, cells were washed twice with PBS and harvested in 100 μl of sample buffer. Samples were then further processed as described before [13] and probed with anti-GFP (Roche) antibody.

Annexin V assay. Twenty-four hours after infection or transfection of HUVECs, apoptosis was induced for 12–24 h. Cells were then collected by mild trypsinization and briefly centrifuged together with the culture supernatant. The cell pellet was washed, resuspended, and stained with PI (1 ug/ml) and Annexin V AlexaFluor488 (Molecular Probes, http://probes.invitrogen.com) or Annexin V APC (Alexis, http://www.axxora.com). The total apoptotic population was determined by analyzing Annexin V–positive and PI-negative/positive cells with a FACSCalibur flow cytometer (BD Biosciences, http://www.bdbiosciences.com). Prior to determining the apoptotic population, transfected cells were gated by their positive GFP signal.

Transfection and immunocytochemistry. HEK293T cells were transfected for 30 h with different GFP-Bep fusion constructs, fixed with 3.7% paraformaldehyde, and immunocytochemically stained with Texas Red–labeled WGA (Invitrogen, http://www.invitrogen.com). Specimens were analyzed by confocal microscopy as described [12].

Determination of IL-8 secretion. The infection (MOI = 300) of HUVECs and the determination of IL-8 secretion by IL-8 DuoSet ELISA kit (R&D Systems, http://www.rndsystems.com) were performed as described before [12].

Determination of intracellular cAMP level. After infection (MOI = 150) of HUVECs for 30 h in 24-well plates, cells were washed with pre-warmed PBS and lysed. Intracellular cAMP level was determined by the EIA system (Biotrak, Amersham) as described by the manufacturer.

Real-time PCR. To quantify the activation of the cAMP pathway, total cellular RNA was isolated at 54 h after infection as described above. RNA manipulation and real-time PCR was performed as previously described [56] using primers listed in Table 2.

Effects of exogenous cAMP and cAMP-elevating agents. HUVECs were infected in the absence or presence of either forskolin (Sigma-Aldrich) and IBMX (Sigma-Aldrich) or dibutyryl cAMP (Sigma-Aldrich) for 24 h with the indicated *Bh* strains (MOI = 300) or left uninfected (control). Apoptosis was induced, and caspase-3/-7 activities were monitored as described above.

CTL assay upon infection. Confluent HLA-A2-positive HUVEC (a gift from B. C. Biedermann, Department of Research, University Hospital Basel, Basel, Switzerland) monolayers were labeled with 5 μM carboxyfluorescein diacetate, succinimidyl ester (CFSE, Molecular Probes), in M199 without FCS according to the manufacturer's protocol. Cells were then infected with indicated *Bh* strains (MOI = 300) or left uninfected in M199/10% FCS/500 μM IPTG for 24 h. The HLA-A2-restricted CTL clones specific to the Y-chromosome-encoded, male-specific minor histocompatibility peptide antigen SMCY were generated as described previously [32]. CTLs were washed by centrifugation and were added in an effector-to-target cell ratio of 5:1 in replacing the infection medium with CTL assay medium (M199, 2% FCS, 500 μM IPTG). Plates were centrifuged to bring the cells in contact. To quantify the surviving and dead cell rate, we used Annexin V and PI staining and flow cytometry (described above). Prior to determining the surviving and dead cell populations, CFSE-positive cells were gated by their positive GFP signal.

Supporting Information

Accession Numbers

The GenBank (http://www.ncbi.nlm.nih.gov/Genbank) accession numbers for orthologous sequences to *Bh* BepA are *Bq* (NC 005955) and *Bt* (CAD37389).

Acknowledgments

We are grateful to M. Quebatte for excellent technical assistance in performing real-time PCR. We also thank Dr. Henri Saenz and Dr. Gunnar Schröder for critical reading of the manuscript. The Bruderholzspital Basel is acknowledged for providing human umbilical cords.

Author contributions. CD conceived and designed the experiments. MCS, FS, MD, and NBD performed the experiments. MCS, FS, MD, and CD analyzed the data. RS, PG, CSC, and BB contributed reagents/materials/analysis tools. MCS and CD wrote the paper.

Funding. This work was supported by grant 3100–06177700 from the Swiss National Science Foundation and grant 55005501 from the International Research Scholar program of the Howard Hughes Medical Institute, as well as a student fellowship from the Misrock Foundation in Basel.

Competing interests. The authors have declared that no competing interests exist.

References

1. Weinrauch Y, Zychlinsky A (1999) The induction of apoptosis by bacterial pathogens. Annu Rev Microbiol 53: 155–187.
2. Hersh D, Monack DM, Smith MR, Ghori N, Falkow S, et al. (1999) The *Salmonella* invasin SipB induces macrophage apoptosis by binding to caspase-1. Proc Natl Acad Sci U S A 96: 2396–2401.
3. Hilbi H, Moss JE, Hersh D, Chen Y, Arondel J, et al. (1998) *Shigella*-induced apoptosis is dependent on caspase-1 which binds to IpaB. J Biol Chem 273: 32895–32900.
4. Fischer SF, Vier J, Kirschnek S, Klos A, Hess S, et al. (2004) *Chlamydia* inhibit host cell apoptosis by degradation of proapoptotic BH3-only proteins. J Exp Med 200: 905–916.
5. Clifton DR, Goss RA, Sahni SK, van Antwerp D, Baggs RB, et al. (1998) NF-kappa B-dependent inhibition of apoptosis is essential for host cell survival during *Rickettsia rickettsii* infection. Proc Natl Acad Sci U S A 95: 4646–4651.
6. Massari P, Ho Y, Wetzler LM (2000) *Neisseria meningitidis* porin PorB interacts with mitochondria and protects cells from apoptosis. Proc Natl Acad Sci U S A 97: 9070–9075.
7. Muller A, Gunther D, Dux F, Naumann M, Meyer TF, et al. (1999) Neisserial porin (PorB) causes rapid calcium influx in target cells and induces apoptosis by the activation of cysteine proteases. EMBO J 18: 339–352.
8. Muller A, Rassow J, Grimm J, Machuy N, Meyer TF, et al. (2002) VDAC and the bacterial porin PorB of *Neisseria gonorrhoeae* share mitochondrial import pathways. EMBO J 21: 1916–1929.
9. Dehio C (2005) *Bartonella*-host-cell interaction and vascular tumour formation. Nat Rev Microbiol 3: 621–631.
10. Kirby JE, Nekorchuk DM (2002) *Bartonella*-associated endothelial prolifer-

ation depends on inhibition of apoptosis. Proc Natl Acad Sci U S A 99: 4656–4661.
11. Kirby JE (2004) In vitro model of *Bartonella henselae*-induced angiogenesis. Infect Immun 72: 7315–7317.
12. Schmid MC, Schulein R, Dehio M, Denecker G, Carena I, et al. (2004) The VirB type IV secretion system of *Bartonella henselae* mediates invasion, proinflammatory activation and antiapoptotic protection of endothelial cells. Mol Microbiol 52: 81–92.
13. Schulein R, Guye P, Rhomberg TA, Schmid MC, Schroder G, et al. (2005) A bipartite signal mediates the transfer of type IV secretion substrates of *Bartonella henselae* into human cells. Proc Natl Acad Sci U S A 102: 856–861.
14. Schroder G, Dehio C (2005) Virulence-associated type IV secretion systems of *Bartonella*. Trends Microbiol 13: 336–342.
15. Cascales E, Christie PJ (2003) The versatile bacterial type IV secretion systems. Nat Rev Microbiol 1: 137–149.
16. Schulein R, Dehio C (2002) The VirB/VirD4 type IV secretion system of *Bartonella* is essential for establishing intraerythrocytic infection. Mol Microbiol 46: 1053–1067.
17. Kawamukai M, Matsuda H, Fujii W, Nishida T, Izumoto Y, et al. (1988) Cloning of the *fic-1* gene involved in cell filamentation induced by cyclic AMP and construction of a delta *fic Escherichia coli* strain. J Bacteriol 170: 3864–3869.
18. Dehio C, Meyer M, Berger J, Schwarz H, Lanz C (1997) Interaction of *Bartonella henselae* with endothelial cells results in bacterial aggregation on the cell surface and the subsequent engulfment and internalisation of the bacterial aggregate by a unique structure, the invasome. J Cell Sci 110: 2141–2154.
19. Sory MP, Cornelis GR (1994) Translocation of a hybrid YopE-adenylate cyclase from *Yersinia enterocolitica* into HeLa cells. Mol Microbiol 14: 583–594.
20. Nagai H, Cambronne ED, Kagan JC, Amor JC, Kahn RA, et al. (2005) A C-terminal translocation signal required for Dot/Icm-dependent delivery of the *Legionella* RalF protein to host cells. Proc Natl Acad Sci U S A 102: 826–831.
21. Alsmark CM, Frank AC, Karlberg EO, Legault BA, Ardell DH, et al. (2004) The louse-borne human pathogen *Bartonella quintana* is a genomic derivative of the zoonotic agent *Bartonella henselae*. Proc Natl Acad Sci U S A 101: 9716–9721.
22. Karin M, Lin A (2002) NF-kappaB at the crossroads of life and death. Nat Immunol 3: 221–227.
23. Nishihara H, Kizaka-Kondoh S, Insel PA, Eckmann L (2003) Inhibition of apoptosis in normal and transformed intestinal epithelial cells by cAMP through induction of inhibitor of apoptosis protein (IAP)-2. Proc Natl Acad Sci U S A 100: 8921–8926.
24. Sassone-Corsi P (1998) Coupling gene expression to cAMP signalling: Role of CREB and CREM. Int J Biochem Cell Biol 30: 27–38.
25. Maurice DH, Palmer D, Tilley DG, Dunkerley HA, Netherton SJ, et al. (2003) Cyclic nucleotide phosphodiesterase activity, expression, and targeting in cells of the cardiovascular system. Mol Pharmacol 64: 533–546.
26. Molina CA, Foulkes NS, Lalli E, Sassone-Corsi P (1993) Inducibility and negative autoregulation of CREM: An alternative promoter directs the expression of ICER, an early response repressor. Cell 75: 875–886.
27. Mayr B, Montminy M (2001) Transcriptional regulation by the phosphorylation-dependent factor CREB. Nat Rev Mol Cell Biol 2: 599–609.
28. Cooper DM (2003) Regulation and organization of adenylyl cyclases and cAMP. Biochem J 375: 517–529.
29. Bernot D, Peiretti F, Canault M, Juhan-Vague I, Nalbone G (2005) Upregulation of TNF-alpha-induced ICAM-1 surface expression by adenylate cyclase-dependent pathway in human endothelial cells. J Cell Physiol 202: 434–441.
30. Schildberg FA, Schulz S, Dombrowski F, Minor T (2005) Cyclic AMP alleviates endoplasmic stress and programmed cell death induced by lipopolysaccharides in human endothelial cells. Cell Tissue Res 320: 91–98.
31. Barry M, Bleackley RC (2002) Cytotoxic T lymphocytes: All roads lead to death. Nat Rev Immunol 2: 401–409.
32. Kummer M, Lev A, Reiter Y, Biedermann BC (2005) Vascular endothelial cells have impaired capacity to present immunodominant, antigenic peptides: A mechanism of cell type-specific immune escape. J Immunol 174: 1947–1953.
33. Zychlinsky A, Sansonetti PJ (1997) Apoptosis as a proinflammatory event: What can we learn from bacteria-induced cell death? Trends Microbiol 5: 201–204.
34. Hueffer K, Galan JE (2004) *Salmonella*-induced macrophage death: Multiple mechanisms, different outcomes. Cell Microbiol 6: 1019–1025.
35. Zigangirova NA, Gintsburg AL (2004) [Role of apoptosis in the regulation of the infectious process]. Zh Mikrobiol Epidemiol Immunobiol Nov–Dec: 106–113.
36. Kwon G, Pappan KL, Marshall CA, Schaffer JE, McDaniel ML (2004) cAMP dose-dependently prevents palmitate-induced apoptosis by both protein kinase A- and cAMP-guanine nucleotide exchange factor-dependent pathways in beta-cells. J Biol Chem 279: 8938–8945.
37. Nishihara H, Hwang M, Kizaka-Kondoh S, Eckmann L, Insel PA (2004) Cyclic AMP promotes cAMP-responsive element-binding protein-dependent induction of cellular inhibitor of apoptosis protein-2 and suppresses apoptosis of colon cancer cells through ERK1/2 and p38 MAPK. J Biol Chem 279: 26176–26183.
38. Zhou B, Li F, Chen H, Song J (2005) The modulation of apoptosis by cyclic AMP involves Akt and epidermal growth factor receptor. Int J Biochem Cell Biol 37: 1483–1495.
39. Rossi AG, Cousin JM, Dransfield I, Lawson MF, Chilvers ER, et al. (1995) Agents that elevate cAMP inhibit human neutrophil apoptosis. Biochem Biophys Res Commun 217: 892–899.
40. Orlov SN, Thorin-Trescases N, Dulin NO, Dam TV, Fortuno MA, et al. (1999) Activation of cAMP signaling transiently inhibits apoptosis in vascular smooth muscle cells in a site upstream of caspase-3. Cell Death Differ 6: 661–672.
41. Yusta B, Boushey RP, Drucker DJ (2000) The glucagon-like peptide-2 receptor mediates direct inhibition of cellular apoptosis via a cAMP-dependent protein kinase-independent pathway. J Biol Chem 275: 35345–35352.
42. Martin MC, Dransfield I, Haslett C, Rossi AG (2001) Cyclic AMP regulation of neutrophil apoptosis occurs via a novel protein kinase A-independent signaling pathway. J Biol Chem 276: 45041–45050.
43. Abramovitch R, Tavor E, Jacob-Hirsch J, Zeira E, Amariglio N, et al. (2004) A pivotal role of cyclic AMP-responsive element binding protein in tumor progression. Cancer Res 64: 1338–1346.
44. Martin MC, Allan LA, Lickrish M, Sampson C, Morrice N, et al. (2005) Protein kinase A regulates caspase-9 activation by Apaf-1 downstream of cytochrome c. J Biol Chem 280: 15449–15455.
45. Hippenstiel S, Schmeck B, N'Guessan PD, Seybold J, Krull M, et al. (2002) Rho protein inactivation induced apoptosis of cultured human endothelial cells. Am J Physiol Lung Cell Mol Physiol 283: L830–L838.
46. Watts VJ, Neve KA (2005) Sensitization of adenylate cyclase by Galpha(i/o)-coupled receptors. Pharmacol Ther 106: 405–421.
47. Fuhrmann O, Arvand M, Gohler A, Schmid M, Krull M, et al. (2001) *Bartonella henselae* induces NF-kappaB-dependent upregulation of adhesion molecules in cultured human endothelial cells: Possible role of outer membrane proteins as pathogenic factors. Infect Immun 69: 5088–5097.
48. Ashton-Rickardt PG (2005) The granule pathway of programmed cell death. Crit Rev Immunol 25: 161–182.
49. Keefe D, Shi L, Feske S, Massol R, Navarro F, et al. (2005) Perforin triggers a plasma membrane-repair response that facilitates CTL induction of apoptosis. Immunity 23: 249–262.
50. Adrain C, Murphy BM, Martin SJ (2005) Molecular ordering of the caspase activation cascade initiated by the cytotoxic T lymphocyte/natural killer (CTL/NK) protease granzyme B. J Biol Chem 280: 4663–4673.
51. Biedermann BC, Pober JS (1999) Human vascular endothelial cells favor clonal expansion of unusual alloreactive CTL. J Immunol 162: 7022–7030.
52. Sambrook J, Fritsch EF, Maniatis T (1989) Molecular cloning: A laboratory manual, 2nd edition. Cold Spring Harbor (New York): Cold Spring Harbor Laboratory Press.
53. Tulp A, Verwoerd D, Dobberstein B, Ploegh HL, Pieters J (1994) Isolation and characterization of the intracellular MHC class II compartment. Nature 369: 120–126.
54. Ferrari G, Knight AM, Watts C, Pieters J (1997) Distinct intracellular compartments involved in invariant chain degradation and antigenic peptide loading of major histocompatibility complex (MHC) class II molecules. J Cell Biol 139: 1433–1446.
55. Bradford MM (1976) A rapid and sensitive method for the quantitation of microgram quantities of protein utilizing the principle of protein-dye binding. Anal Biochem 72: 248–254.
56. Dehio M, Quebatte M, Foser S, Certa U (2005) The transcriptional response of human endothelial cells to infection with *Bartonella henselae* is dominated by genes controlling innate immune responses, cell cycle, and vascular remodelling. Thromb Haemost 94: 347–361.
57. Regnery RL, Anderson BE, Clarridge JE 3rd, Rodriguez-Barradas MC, Jones DC, et al. (1992) Characterization of a novel *Rochalimaea* species, *R. henselae* sp. nov., isolated from blood of a febrile, human immunodeficiency virus-positive patient. J Clin Microbiol 30: 265–274.
58. Zhang P, Chomel BB, Schau MK, Goo JS, Droz S, et al. (2004) A family of variably expressed outer-membrane proteins (Vomp) mediates adhesion and autoaggregation in *Bartonella quintana*. Proc Natl Acad Sci U S A 101: 13630–13635.